Asian Transport Studies 8 (2022) 100081

Contents lists available at ScienceDirect

Asian Transport Studies

journal homepage: www.sciencedirect.com/journal/asian-transport-studies

Prediction of travel time on urban road links with and without point detectors

Ang Li [a,*], William H.K. Lam [a], Mei Lam Tam [a], Ren Xin Zhong [b], Wei Ma [a]

[a] Department of Civil and Environmental Engineering, The Hong Kong Polytechnic University, Kowloon, Hong Kong, China
[b] Guangdong Key Laboratory of Intelligent Transportation Systems, School of Intelligent Systems Engineering, Sun Yat-sen University, Guangzhou, China

ARTICLE INFO

Keywords:
Travel time prediction
Functional principal component analysis
Maximum likelihood estimation
Multi-source traffic data

ABSTRACT

This paper proposes a short-term rolling horizon framework for the within-day prediction of travel times on links with and without point detectors (referred to as observed and unobserved links respectively) along a selected path covered in the Hong Kong journey time indication system (JTIS). In Hong Kong JTIS, the number of point detectors on major roads is usually limited due to the financial budget and site constraints in the densely populated urban area. However, the prediction of the travel times on urban road corridors particularly on the links without point detectors is also valuable to road users and traffic authorities. This paper proposes a 2-stage framework based on functional principal component analysis and maximum likelihood estimation method to predict the mean and standard deviation of the travel times on the study path and observed links as well as unobserved links once every 2 min for the next 30 min. An urban road network in Hong Kong is selected as a case study. The prediction results are validated using an independent dataset from JTIS, demonstrating the practical applicability of the proposed framework.

1. Introduction

The increasing deployment of intelligent transportation systems (ITSs) enables road users, traffic managers, and operators to more efficiently access real-time road information. Travel time is a critical indicator of road performance and the level of service (EI Faouzi et al., 2010). As the amount of traffic data obtained from different types of traffic detectors increases, so does the need for network-wide travel time information. Travel time information disseminated by advanced traveler information systems (ATISs) can be categorized into estimated and predicted travel times. The estimated travel time provides en-route information to guide road users on scheduling and route decisions. The predicted travel time delivers pre-route information to increase road network usage efficiency (Mori et al., 2015). According to the predicted travel time information, road users can make decisions on departure time and preferred route for their travel. Both types of travel time information rely on the techniques of travel time estimation and prediction from traffic detector data. The within-day path and link travel time information can be predicted using historical traffic data and real-time traffic detector data (Li et al., 2020; Zhong et al., 2017; Vlahogianni et al., 2014). Travel time uncertainty is an important factor in the short-term travel time prediction problems. The sources of uncertainty can be categorized into traffic demand and transport supply (Shao et al., 2013). Demand uncertainty is related to the day-to-day variations of traffic demand, and supply uncertainty is related to the disturbances in the road network, including traffic accidents and adverse weather conditions. The uncertainty of travel time prediction error, which is related to the prediction models, has significant effects. For predictions based on the estimated travel times, the variance due to estimation error is another source of uncertainty (Li and Rose, 2011). Apart from giving the predicted mean travel times only, ATISs may also provide the variance of travel times, which has been worked out as prediction results in the recent studies (Du et al., 2012; Hofleitner et al., 2012; Zhong et al., 2017).

To capture and monitor the dynamics of path and link travel times, various types of traffic detectors have been developed and installed on roads. There are two major types of traffic detectors (Mori et al., 2015): point and interval detectors. Point detectors, such as loop detectors and video image detectors, are fixed at given locations of the roads. By sensing passing vehicles, they can measure and collect spot speed data and traffic flow data. Interval detectors include probe vehicles, floating cars, and automatic vehicle identification (AVI) detectors such as radio-frequency identification (RFID) tag readers and automatic license

* Corresponding author.
E-mail addresses: ang-leon.li@connect.polyu.hk (A. Li), william.lam@polyu.edu.hk (W.H.K. Lam), trptam@polyu.edu.hk (M.L. Tam), zhrenxin@mail.sysu.edu.cn (R.X. Zhong), wei.w.ma@polyu.edu.hk (W. Ma).

https://doi.org/10.1016/j.eastsj.2022.100081
Received 19 July 2021; Received in revised form 31 March 2022; Accepted 21 June 2022
Available online 29 June 2022

Notations descriptions

External Variables

A	Set of links
D^t	Set of path travel time observations of vehicles that enter the path at time t
$x_i(t)$	ith measurement on path/link travel time at time t

Internal Variables

t, u	Path entry time in the current horizon
h, v	Path entry time in the prediction horizon
$\varphi_w(t)$	Path travel time process of time t on day w
$\mu(t)$	Mean function of path travel times
e	Measurement errors of traffic detectors
$\varphi_k(t)$	Eigenfunction of the kth FPC of time t
ξ_{wk}	Score of the kth FPC on day w
γ_q	Eigenvalue of the qth FPC (prediction horizon)
λ_k	Eigenvalue of the kth FPC (current horizon)
$G_{t,u}$, $G_{h,v}$	Covariance functions of path travel times in the current horizon and prediction horizon
K, Q	Number of FPCs
f, g	Smooth regression functions of FPC scores
x_i^t	The ith observed path travel time of vehicles that enter the path at time t
$\delta_{i,a}$	Link–path incidence indicator
η_a	Proportion of link travel time of link a on the monitored path
μ_a^t	Mean travel time on link a for vehicles that enter the path at time t
σ_a^t	Standard deviation of travel time on link a for vehicles that enter the path at time t
λ	Multiplier in the MLE problem
σ_p^t	Standard deviation of path travel time for vehicles that enter the path at time t
θ_a^t	Information about link a, including the mean and standard deviation of link travel time for vehicles that enter the path at time t
θ^t	Information about links, including the mean and standard deviation of link travel times for vehicles that enter the path at time t

Abbreviations

ALPR	automatic license plate recognition
ARIMA	autoregressive integrated moving average
ATISs	advanced traveler information systems
AVI	automatic vehicle identification
FPC	functional principal component
FPCA	Functional principal component analysis
ITSs	intelligent transportation systems
JTIS	journey time indication system (https://www.td.gov.hk/en/transport_in_hong_kong/its/its_achievements/journey_time_indication_system_/index.html)
LSTM NN	long short-term memory neural network
MAE	mean absolute error
MAPE	mean absolute percentage error
MLE	maximum likelihood estimation
PACE	principal analysis by conditional expectation
PCA	Principal Component Analysis
RFID	radio-frequency identification
RMSE	root mean square error
SMP	speed map panel (https://www.td.gov.hk/en/transport_in_hong_kong/its/its_achievements/speed_map_panels/index.html)
TTD	Path-based travel time decomposition

plate recognition (ALPR) cameras. They can directly measure and collect the vehicular travel time data of the road segments under observation. Point detectors efficiently capture and monitor the temporal evolution of traffic conditions near their locations. At the locations installed with point detectors, the vehicle flow rate and the mean speed and standard deviation of vehicle spot speeds are collected at pre-determined time intervals. AVI detectors provide better spatial coverage on road segments along the monitored path; thus, the spatial information of travel time on the path can be obtained. Although AVI detectors are characterized by a relatively low sampling rate, they directly capture the travel times of individual vehicles. By processing point detector data, AVI data, and offline estimates of path travel times, the Hong Kong journey time indication system (JTIS;//www.td.gov.hk/en/transport_in_hong_kong/its/its_achievements/journey_time_indication_system_/index.html) can provide **instantaneous path travel time estimates** every 2 min.

The multiple traffic data sources provide a broad platform for investigating travel time estimation and prediction problems. For example, speed-based models can estimate travel times from speed data collected by point detectors (Xiao, 2011). The estimated travel times further provide a basis for further predictions. Travel time can be directly extracted from the AVI system database. However, a filtering process is usually required to remove the outliers because vehicles may stop or detour along the paths (Soriguera and Robusté, 2011; Tam and Lam, 2011; Dion and Rakha, 2006). Owing to the uncertain sampling rate and the sparsely distributed sample points associated with probe vehicle data such as GPS data, the spot speeds reported by vehicles or travel times manipulated for short detection segments should be further investigated (Zhong et al., 2017; Yin et al., 2015; Hofleitner et al., 2012).

When both the path travel time estimates from **JTIS** and the **point detector data** are available, the research question can be extended to tackle more challenging path-based travel time decomposition (TTD) problems for estimation and/or prediction on the links with and without detectors along the study path. The path-based travel time information can be obtained from JTIS estimates (referred to as the path travel time estimates in this paper). The travel time information on links with point detectors can be observed and analyzed directly for the link travel time estimation and prediction. Owing to budget constraints, the travel time information on links without point detectors along the path is not observed; however, it is still valuable to road users. In this paper, links with point detectors are referred to as observed links, whereas those without point detectors are referred to as **unobserved** links along the same path. Using a static travel time estimation model, Shao et al. (2018) fused AVI and point detector data to estimate the mean and variance of instantaneous travel times on the unobserved links. To satisfy the ATIS requirements, the static model can be extended to the dynamic model for predicting the mean travel times on the path and links and their travel time variations. Table 1 shows that relevant studies have mainly investigated the prediction of within-day travel times on observed links and/or paths with detected data. However, the prediction of the travel times on unobserved links along the study path is equally valuable to road users. To capture the dynamics of the travel times on unobserved links, spot speed information from point detectors and JTIS estimates should be fused and analyzed. Therefore, there is a need to develop a path-based travel time decomposition framework for predicting the variations in the travel times on the path, observed links, and unobserved links by using limited point detector data and JTIS estimates.

Several techniques for short-term traffic prediction were developed in the past decade and have since matured. Most of these techniques can be categorized into traffic theory-based (or model-based) and data-

Table 1
Comparison of travel time prediction studies in literature.

Author	Travel times of			Travel time variations of			Data sources
	path	observed links	unobserved links	path	observed links	unobserved links	
Du et al. (2012)	×	✓	×	×	✓	×	Simulated link travel time
Hofleitner et al. (2012)	✓	×	×	✓	×	×	GPS data
Yildirimoglu and Geroliminis (2013)	✓	×	×	×	×	×	Point detector data
Soriguera and Robusté (2011)	✓	×	×	×	×	×	AVI and point detector data
Zhong et al. (2017)	✓	✓	×	✓	✓	×	GPS data
This study	✓	✓	✓	✓	✓	✓	JTIS data and point detector data

driven approaches (Mori et al., 2015). Traffic theory-based models predict traffic scenarios and travel times by generating future traffic conditions (Papageorgiou et al., 2010; Celikoglu, 2007). However, these models may simplify some realistic features of traffic conditions in the simulation process; therefore, the traffic condition prediction performance is limited. Data-driven approaches are either parametric or non-parametric. Parametric approaches, such as linear regression, Bayesian network, and time-series models, have a more logical structure and comprehensive mathematical foundation. However, they are computationally expensive and cannot effectively handle nonlinear data in reality (Gu et al., 2020; Li et al., 2020; Fusco et al., 2016; Du et al., 2012). Traffic prediction based on non-parametric approaches often involves families of neural networks, decision trees, support vector regression, and other local regression models (Cui et al., 2020; Li et al., 2020; Feng et al., 2019). Moreover, compared with parametric approaches, the calibration process of various parameters is avoided. The non-parametric models can handle nonlinear data but involve black-box procedures (Vlahogianni et al., 2014; Li and Rose, 2011). Moreover, the training models are site-specific and need further training for other locations.

Functional principal component analysis (FPCA), a statistical tool for functional data analysis, is an extension of principal component analysis that has been frequently applied in the transportation sector. The traffic variables are regarded as stochastic processes to be imputed, estimated, and predicted during the FPCA process. As an extension of Principal Component Analysis (PCA), FPCA has been tested and deemed suitable for traffic data analysis. Chiou (2012) and Chiou et al. (2014) performed FPCA to cluster traffic flow patterns, impute missing traffic flow values, detect outliers, and predict traffic flows. Guardiola et al. (2014) monitored and recognized traffic patterns by applying FPCA to traffic flow data. Chen and Müller (2014) applied FPCA to GPS data to predict vehicle speed distribution. Zhong et al. (2020, 2017) achieved satisfactory results on the prediction and estimation of link travel time variations. These works demonstrate the merits of FPCA in reducing the dimensionality of traffic data without compromising their original integrity.

The path-based travel time decomposition (TTD) problem is defined to decompose a complete corridor or path travel time to travel times on sub-links. Models such as hidden Markov models and Gaussian mixture models are used to estimate the path-based travel times with decomposition on links along the path with AVI data (Yang et al., 2018; Yin et al., 2015). Other TTD approaches are based on assumptions related to the inter-relationships of travel times on links along the study path, such as variance–covariance temporal relationship between observed and unobserved links (Shao et al., 2018; Yin et al., 2015; Hellinga et al.,). These approaches outperform the simple proportional allocation approach (e.g., those that allocate link travel times according to link lengths on the basis of the distance-based path travel time decomposition).

This paper addresses the within-day travel time prediction problems by proposing a 2-stage prediction framework for predicting the mean and standard deviation of travel times on the study path, observed links, and unobserved links. The path and links are within a road corridor that deploys a traffic detector system, including AVI and point detectors. Hence, the JTIS estimates are obtained from AVI and point detector data. In principle, point detectors can detect all passing vehicles. Owing to the large data flow, the database of the point detector system usually stores the aggregated speed information at specific time intervals, rather than individual vehicle records.

In this paper, path-level within-day travel time variability obtained from JTIS data and link-level within-day travel time variability obtained from point detector data are modeled through FPCA. The FPCA process is included in stage 1 of the proposed prediction framework. With the predicted travel time variations of the path and observed links, the travel time variations of unobserved links are predicted through the formulation of a maximum likelihood estimation (MLE) problem. With the concept of TTD (Wang, 2015; Yin et al., 2015), the travel time variations of unobserved links are predicted under conditional information obtained from stage 1 of the proposed prediction framework. This TTD process is included in stage 2 of the proposed prediction framework.

The rest of this paper is organized as follows: Section 2 presents the preliminaries and a notation list for all the variables and abbreviations used in this paper. Section 3 demonstrates the proposed 2-stage framework for predicting the mean and standard deviation of travel times on the study path as well as the observed links and unobserved links, based on the application of FPCA and MLE in stages 1 and 2 respectively. Section 4 presents the performance of the proposed prediction framework through an empirical study. Section 5 provides the conclusions.

2. Preliminaries

Symbols with a '•' superscript are referred to the "estimated" variables rather than the measured or observed variables.

3. Methodology

3.1. FPCA for predicting travel time on path and observed links

As with the other traffic variables mentioned in Section 1, travel time has stochastic features, especially due to non-recurrent incidents. Studies have investigated the effects of non-recurrent incidents on the stochasticity of traffic conditions (Zhong et al., 2017, 2020; Lam et al., 2008). Regarding the link and path travel times as stochastic processes, two sets of FPCA models have been established for analyzing the captured path and link travel times as functional data. The model describing the process for path travel times and observed link travel times are similar; thus, only the modeling process of path travel time is introduced here. According to the Karhunen–Loève expansion, the stochastic process of path travel time can be expressed as (1) if the number of functional principal components is determined to be K. The path travel time function is expressed as the summation of the mean functions of path travel times and variations. The variations are explained by the summation of the products of functional principal component (FPC) scores and eigenfunctions of all of the functional principal components. (1) holds for all the periods in both current and prediction horizons. The mean and covariance functions of the path travel times are expressed as (2) and (3), respectively. The covariance function is expressed as an orthogonal expansion (in the L2 space) obtained from the summation of

the product of the non-increasing eigenvalues and the eigenfunctions of each FPC. The FPC scores in (1) and (3) satisfy (4) and (5). Furthermore, the path travel time provided by JTIS estimates is modeled in (6). It is assumed that the measurement error e is independently and identically distributed with an expectation of zero and the same variance as that of the measurements. The error e can also be referred to as the difference between any measurement and the corresponding path travel time function at a specific time of day.

$$\varphi_d(t) = \mu(t) + \sum_{k=1}^{K} \xi_{dk}\varphi_k(t) \tag{1}$$

$$\mu(t) = E(\varphi(t)) \tag{2}$$

$$G(t,u) = \sum_{k=1}^{K} \lambda_k \varphi_k(t)\varphi_k(u) \tag{3}$$

$$E(\xi_k) = 0 \tag{4}$$

$$Var(\xi_k) = \lambda_k \tag{5}$$

$$x_i(t) = \mu(t) + \sum_{k=1}^{K} \xi_k\varphi_k(t) + e \tag{6}$$

When the path travel time estimates from JTIS are available, the estimation procedure using $\mu(t)$, λ_k, $\varphi_k(t)$, and ξ_{dk} is the first step of the FPCA process. The estimation procedures are detailed in the literature (Zhong et al., 2017; Chen and Müller, 2014; Yao et al., 2005). The path travel time with the error term is obtained from AVI data. The FPC score is estimated through the principal analysis by conditional expectation (PACE) method; the corresponding procedure is also mentioned in the literature. According to Ji and Müller (2017), the PACE method can provide the best predictor under the Gaussian assumption. Thus, the conditional predicted path travel times can be assumed to be Gaussian-distributed to simplify the prediction problem. Generally, the number of FPCs can be determined using one of three criteria: the fraction of variance explained, Akaike information criterion, or Bayesian information criterion, depending on the data features.

The path travel time process in the current horizons and prediction horizons are denoted as $\varphi(t)$ and $\varphi(h)$, respectively. The numbers of FPCs for these horizons are K and Q, respectively. The path travel time functions in the current and prediction horizons can be obtained after the first step of FPCA. They are expressed as (7) and (8), respectively. Both equation models are trained with input data and correlated through FPCA for prediction. For the FPCA-based prediction process, the additive conditional expectation and variance models, expressed as (9) and (10), respectively, are adopted as in previous approaches (Zhong et al., 2017; Chen and Müller, 2014; Müller and Yao, 2008). The eigenvalues γ_q and FPC scores in the conditional modeling satisfy (11) and (12). In these two equations, f and g are smooth regression functions of FPC scores. They are calibrated using locally weighted least squares regression and cross-validation based on corresponding scatterplots. The details are available in Zhong et al. (2017) and Chen and Müller (2014). For the prediction process, the FPC scores are estimated and updated as $\xi_k^{'}$; then, the predicted mean and covariance function can be determined as (13) and (14), respectively.

$$\hat{\varphi}(t) = \hat{\mu}(t) + \sum_{k=1}^{K} \hat{\xi}_k \hat{\varphi}_k(t) \tag{7}$$

$$\hat{\varphi}(h) = \hat{\mu}(h) + \sum_{q=1}^{Q} \hat{\xi}_q \hat{\varphi}_q(h) \tag{8}$$

$$\hat{E}(\varphi(h)|\varphi(t)) = \hat{\mu}(h) + \sum_{q=1}^{Q}\Big(\sum_{k=1}^{K} \wedge f_{qk}(\xi_k)\Big)\hat{\varphi}_q(h) \tag{9}$$

$$\hat{C}ov(\varphi(h),\varphi(v)|\varphi(t)) = \sum_{q=1}^{Q}\Big(\hat{\gamma}_q + \sum_{k=1}^{K}\big(\hat{g}_{qk}(\xi_k) - \hat{f}^{2}_{\ qk}(\xi_k)\big)\varphi_q(h)\varphi_q(v) \tag{10}$$

$$E(\xi_q) = 0 \tag{11}$$

$$Var(\xi_k) = \gamma_q \tag{12}$$

$$\hat{E}(\varphi(h)|\varphi(t)) = \hat{\mu}(h) + \sum_{q=1}^{Q}\Big(\sum_{k=1}^{K} \wedge f_{qk}(\xi_k^{'})\Big)\hat{\varphi}_q(h) \tag{13}$$

$$\hat{C}ov(\varphi(h),\varphi(v)|\varphi(t)) = \sum_{q=1}^{Q}\Big(\hat{\gamma}_q + \sum_{k=1}^{K}\big(\hat{g}_{qk}(\xi_k^{'}) - \hat{f}^{2}_{\ qk}(\xi_k^{'})\big)\varphi_q(h)\varphi_q(v) \tag{14}$$

3.2. MLE for predicting travel time on unobserved links

Given that stochastic travel time information for unobserved links is unknown, fusing the relevant information provided by JTIS estimates and point detectors is necessary to obtain the travel time variations of unobserved links. The travel time variations of the path and observed links are predicted according to the JTIS estimates and point detector data, respectively. These predicted values are outputs of stage 1 and inputs of stage 2 in the proposed prediction framework. With the predicted travel time information, the relationships between travel times on a path, observed links, and unobserved links can be found via an optimization process. The MLE problem is formulated through the trip-splitting approach, which was proposed by Yin et al. (2015), rather than through parameter estimation based on assumed travel time distributions. The maximization of the log-likelihood will result in an iterative process for obtaining the travel time variations of unobserved links. According to Yin et al. (2015) and Wang (2015), the trip-splitting approximation approach avoids the expensive computation spent on the integral of the conditional probability density function. It is assumed that the proportions of the travel times on links to that on the whole monitored path vary only slightly. Moreover, as both the path and link travel times are time-dependent, the experienced path travel times are modeled from individual link travel time functions via an approach similar to that proposed by Zhong et al. (2017). To estimate the predicted information of unobserved links, an MLE problem is formulated as (15). The constraints (16) and (17) are the properties of the proportion values. Because the FPCA process assumes Gaussian distributions of conditional travel time, the problem can be solved using Lagrange multipliers, as derived by Yin et al. (2015). The mean and standard deviation of link travel time variations along the monitored path can be expressed as (18) and (19): the derivative of (15) with respect to the mean and standard deviation is calculated and set to zero. The multiplier and proportion values can be solved by using (20) and (21). They are time-dependent within the rolling horizon scheme, described in the following section.

$$\underset{\theta^t,\eta}{Maximize}: LL(\theta^t,\eta|D^t) = \sum_{i\in D^t}\sum_{a\in A}\delta_{p,a}\log f_a(\eta_a x_i^t;\theta_a^t) \tag{15}$$

$$\sum_a \eta_a = 1 \tag{16}$$

$$0 \le \eta_a \le 1 \tag{17}$$

$$\mu_a^t = \frac{\sum_{i \in D^t} \delta_{i,a} \eta_a x_i^t}{\sum_{i \in D^t} \delta_{i,a}} \tag{18}$$

$$\sigma_a^t = \frac{\sum_{i \in D^t} \delta_{i,a} (\eta_a x_i^t - \mu_a^t)^2}{\sum_{i \in D^t} \delta_{i,a}} \tag{19}$$

$$\lambda = \frac{\sum_{i \in D^t} x_i^t (x_i^t - \sum_{a \in A} \delta_{i,a} \mu_a^t)}{\sum_{a \in A} \delta_{p,a} \sigma_a^{t2}} \tag{20}$$

$$\eta_a = \mu_a^t \frac{\sum_{i \in D^t} x_i^t}{\sum_{i \in D^t} x_i^{t2}} + \lambda \frac{\sigma_a^{t2}}{\sum_{i \in D^t} x_i^{t2}} \tag{21}$$

To solve the above problem, an efficient iterative algorithm is adapted from the expectation–maximization algorithm (Yin et al., 2015). The mean and standard deviation of travel times on all considered links are first initialized. Then, the multiplier and proportion values can be obtained using (20) and (21). The mean and the standard deviation of travel times on all considered links can be updated according to the calculated proportions. The log-likelihood can be evaluated according to (16). The process will continue until the convergence of the log-likelihood or involved parameters.

3.3. Prediction framework and rolling horizon scheme

A 2-stage prediction framework is proposed in this paper. For each prediction process, FPCA models are initially applied to obtain the travel time variations of the path and observed links according to the current and historical JTIS estimates and point detector data. The formulated MLE problem is solved through optimization to obtain the predicted travel time information on the unobserved links.

The rolling horizon scheme as shown in Fig. 1 is adopted to achieve better prediction performance. This scheme has been used in studies on travel time estimation and prediction for several years (Zhong et al., 2017; Lu et al., 2018; Pan et al., 2013; Yin et al., 2002). It can be noted in Fig. 1 that each cycle contains the current horizon (represented by the left line of each horizon) and the prediction horizon (represented by the right line of each horizon). The rolling horizon of the proposed 2-stage prediction framework is moved according to the size of the rolling step (represented by green dotted lines). The maximum scale of travel times and the frequency of travel time information dissemination through ATISs are considered in the horizon selection. The predicted information for time intervals within the prediction horizon is updated several times depending on the size of the rolling step and the length of the prediction horizon. Road users can adjust their route choices and departure times according to the frequently updated prediction information. Sensitivity tests on the cycle length were conducted in the case study below.

4. Empirical study

4.1. Relevant ITS projects in Hong Kong

In this section, the relevant ITS projects in Hong Kong are first introduced to provide an overview of the traffic data adopted in the case study. The JTIS and speed map panel (SMP) system are representative ITS projects deployed in Hong Kong (Fig. 2). JTIS provides path travel time information on major routes for travel crossing the harbour by alternative tunnels between Hong Kong Island and Kowloon urban area, and SMP provides the path travel time and sectional speed information in the strategic road network of the New Territories of Hong Kong. In these two systems, the sectional speeds are presented in three colors to reflect the different traffic conditions. The path travel times and sectional speeds are estimated from traffic data collected from AVI detectors and point detectors and updated every 2 min.

Two types of traffic detectors, AVI and point detectors, are deployed in these two ITS projects. For point detectors, both projects adopt video image detectors to collect speed and flow data. For AVI detectors, JTIS uses RFID tag readers, while SMP uses ALPR cameras for AVI data collection. A preliminary study found that RFID tag readers collect fewer AVI records in the New Territories than in Hong Kong Island and

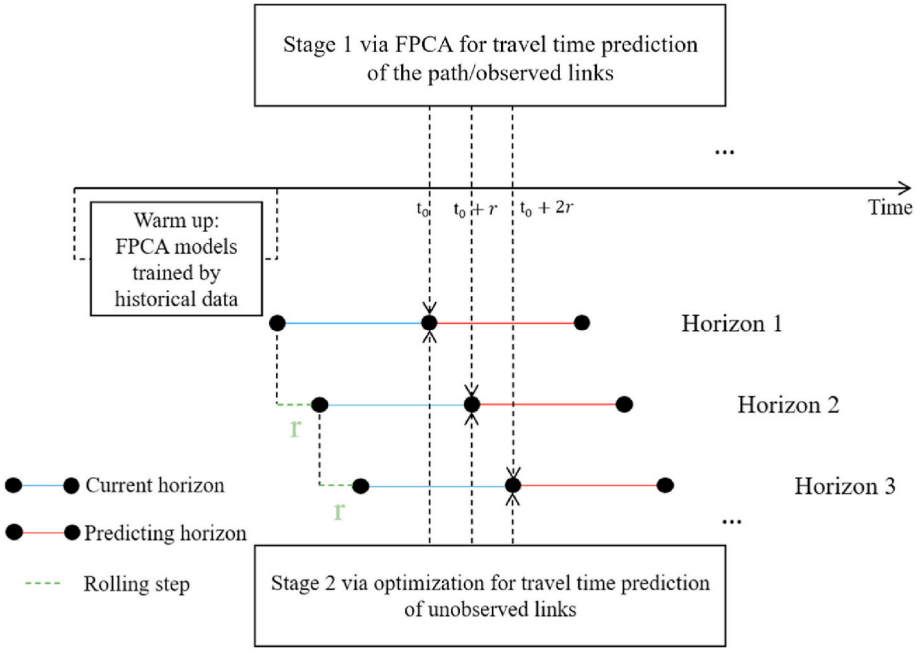

Fig. 1. The rolling horizon scheme.

(a) JTIS (b) SMP

Fig. 2. The JTIS and SMP in Hong Kong.

Kowloon urban areas. Thus, to collect more samples for travel time/speed estimation, the SMP project adopts ALPR technology. AVI detectors detect only commercial vehicles (vehicles registered by companies) with privacy concerns. Moreover, the license plate information of commercial vehicles would not be stored in the AVI database to protect the privacy of the drivers and vehicles.

Previous validation studies on both JTIS and SMP have found that both systems can provide reliable path travel time estimates to road users in Hong Kong, although the numbers of traffic detectors in the studies were limited (Tam and Lam, 2008, 2011). However, JTIS and SMP only provide instantaneous travel time/speed estimates, but not the predicted travel time information. To enrich the travel time information provided by ATISs in Hong Kong, providing travelers with predicted travel time information for pre-trip planning is vital.

4.2. Case study

A path of the Hong Kong urban road network is chosen and shown in Fig. 3 for the case study in this paper. The **9.2 km** path spans from the Island Eastern Corridor in Hong Kong Island to the Western Harbour Crossing in Kowloon urban area. The links along the path are defined based on the road features as well as the detection zone of point detectors installed along the roads. Point detectors are installed in seven links (referred to as observed links) along the path, and seven links are without point detectors (referred to as unobserved links). The free-flow path travel time is **8.39 min**, and the average free-flow speed traveling along the path is 65.8 km/h. A pair of AVI detectors are located at the path entry and exit. The study path location is illustrated in Fig. 3 together with the detector locations. Both the observed links (links 1, 3, 5, 6, 8, 11, 12) and unobserved links (links 2, 4, 7, 9, 10, 13, 14) are marked on the location map. Observed link 6 (i.e. OL6 in Fig. 3), which is regarded as an unobserved link for validation, is underlined.

The JTIS and point detector datasets for November 2017 are adopted as this month has no public holidays and more weekdays. There are 22 weekdays in November 2017, **excluding weekends and public holidays**. The data from 7:00 to 23:00 are adopted for the case study. The JTIS provides the mean of the path travel time estimates once every 2 min. The point detector data consists of the mean and variance of vehicular speed at **2 min** intervals. However, the data for some time intervals may be missing. Thus, an imputation process is performed to ensure the completeness of the speed dataset. To validate the prediction performance in this case study, the JTIS path-based dataset for November 29, 2017 (Wednesday), and mean link-level speed data collected by point detectors are adopted as the ground truth. The average speeds along the path and links are calculated from the distance and travel time on the path and links, respectively. The travel time prediction process follows the rolling horizon scheme, as mentioned in Section 3. The prediction framework is evaluated according to the most updated information provided by the framework, as shown in Fig. 4. For example, it can be observed in Fig. 4 that when the prediction horizon contains the prediction results for the next 8 min, only the prediction results for the first 2 min (represented by the first short line cut by dotted lines in each horizon) are to be compared with the actual path or link travel times (represented by the top line). In this way, the prediction

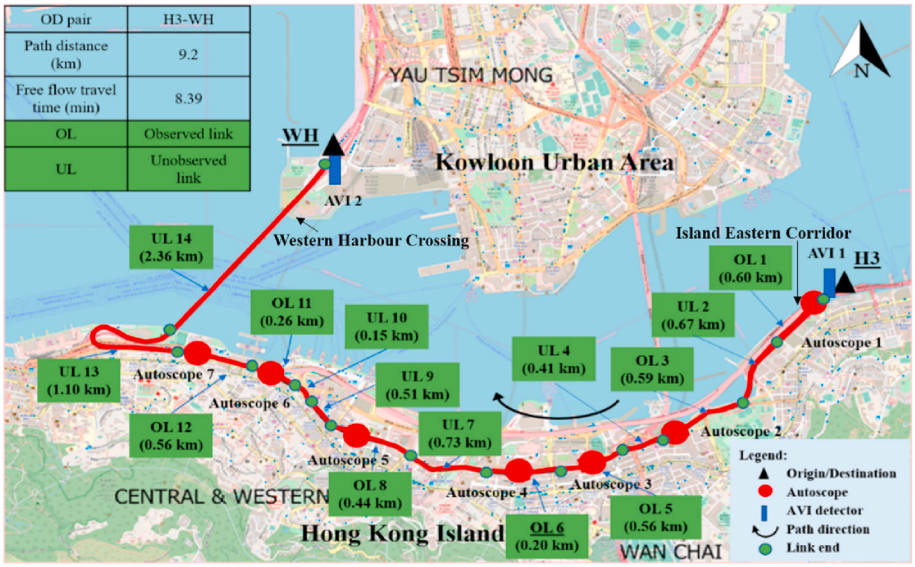

Fig. 3. Map of the study path.

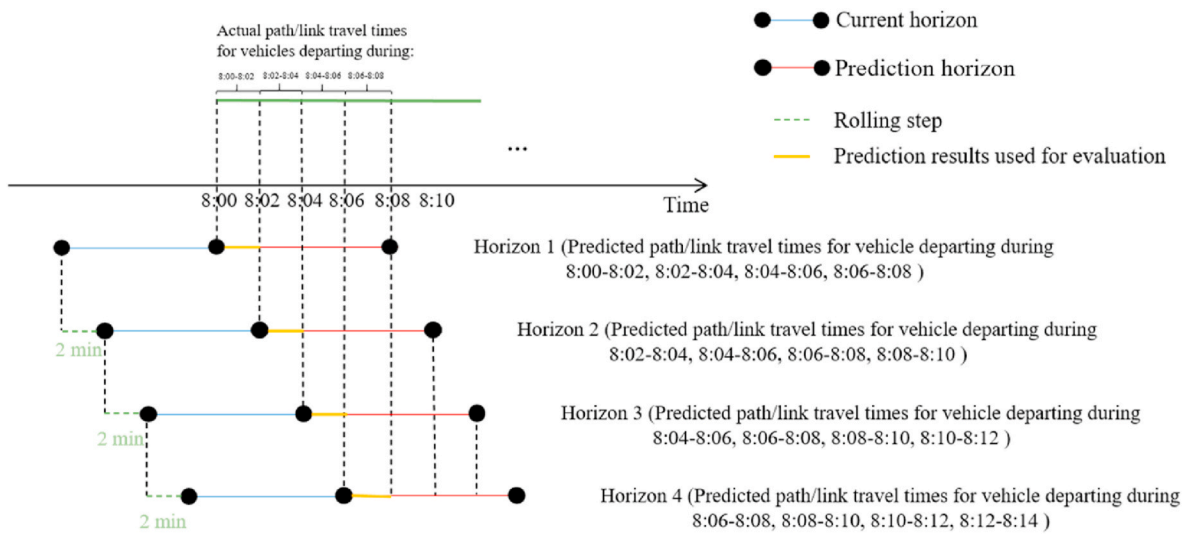

Fig. 4. Example of performance evaluation of rolling horizon.

framework can achieve higher accuracy.

In addition, a sensitivity test on the length of the prediction horizon is performed using the dataset of the path travel times in this case study. As the length of the prediction horizon is set to be equal to the length of the current horizon, the sensitivity test results for the cycle length and rolling step can be obtained for comparison. The prediction performance is evaluated in terms of the mean absolute percentage error (MAPE). The evaluation results are presented in Fig. 5. It can be found in Fig. 5 that the prediction accuracy decreases with an increase in the prediction horizon and rolling step.

For the following experiments, we select the values of the rolling step and prediction horizon based on the rate of change of MAPE by the rolling step and prediction horizon, which is 0.06%/min and 0.36%/min, respectively. Therefore, reducing the rolling step has better efficiency than reducing the prediction horizon. The value of the rolling step is set to be 2min. A trade-off exists between prediction accuracy and ATIS information richness. When the prediction horizon length is small, the ATIS-provided information is limited. Moreover, when ATIS information richness (represented by prediction horizon) is relatively large, the loss of prediction accuracy is faster (from 0.06%/min to 0.17%/min with a 20 min change of prediction horizon in Fig. 5). Therefore, the prediction horizon is set to be 30 min, which balances the prediction accuracy (5.4% of MAPE) and ATIS information richness.

The JTIS estimates and point detector data for the past 30 min are used to predict the travel time information for the subsequent 30 min at each step. The rolling step is 2 min, which means that prediction occurs every 2 min. The predicted travel time information is updated once every 2 min. Through the data analysis of travel time variations, November 29, 2017 (Wednesday) is chosen for validation because of the larger within-day variations of travel time on that day.

Fig. 6 shows the confidence intervals at levels of 95%, 85%, and 75%, which consists of the predicted means and standard deviations of the path travel times against the ground truth from 07:00 to 23:00. The within-day variations of travel times are captured in Fig. 6. The mean of the observed path travel times falls in the range between 481s and 1454s. It was found in the validation results of the proposed model that there are 98.3% of time intervals with less than 20% of MAPE, which meets the JTIS performance requirement with a 95% chance that the

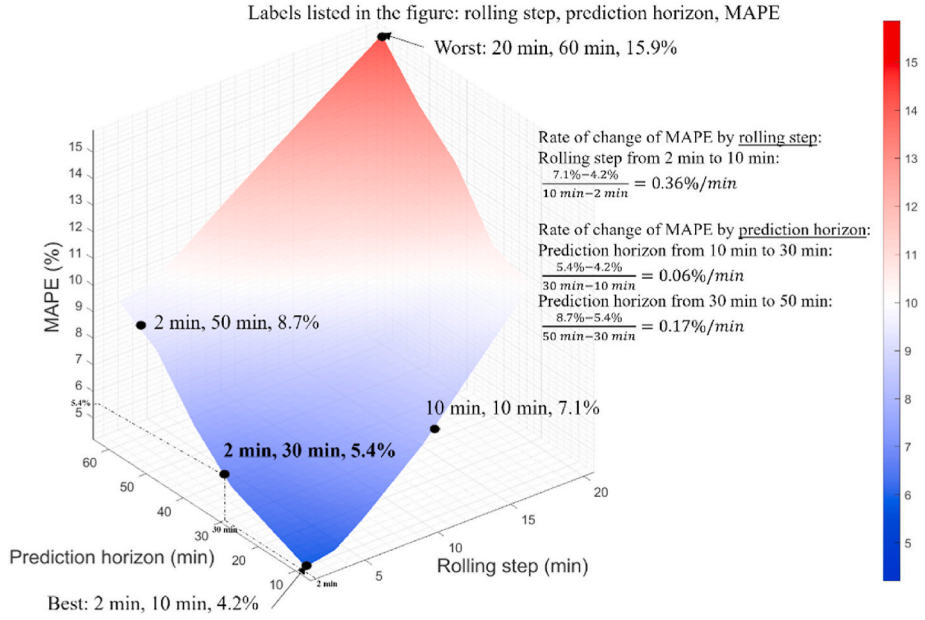

Fig. 5. Sensitivity test results by prediction horizon and rolling step.

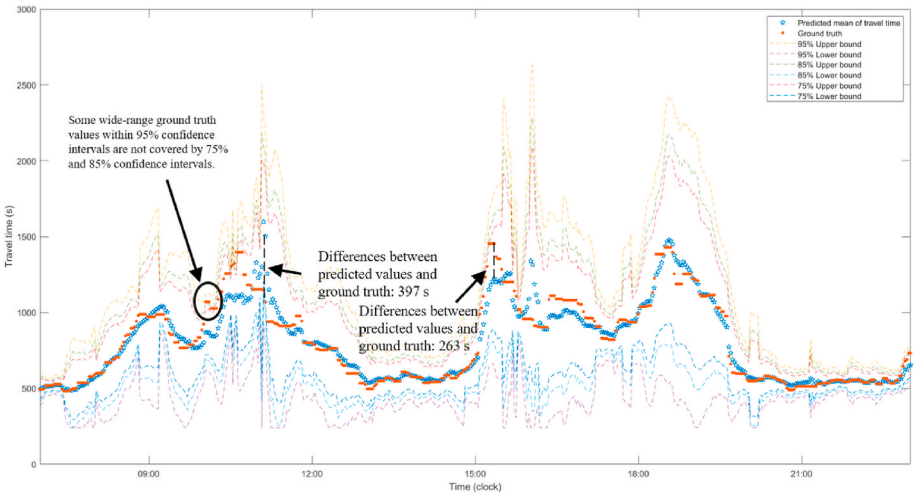

Fig. 6. 75%, 85%, and 95% confidence intervals of predicted path travel times at 7:00–23:00.

estimation errors are not greater than 20% (Tam and Lam, 2008, 2011). The ground truth is within the 95% confidence interval of predicted path travel times. It can be observed in Fig. 6 that some ground truth values within the upper and lower bounds of 95% confidence interval are not covered by that of 75% and 85% confidence intervals. Moreover, the maximum differences between the predicted values and ground truth at 2-min intervals around 11:00 and 15:30 are relatively large: 397s (26%) and 263s (18%), respectively. These errors may be partly due to the larger within-day variations of travel time on that day and should be further investigated in the future study.

For the prediction of travel time variations of the observed link in the case study, the speed data are applied in the FPCA model (alternatively, the converted link travel times from the speed data can be applied in the FPCA model). The predicted speed results are converted to link travel times for stage 2 of the proposed prediction framework. Fig. 7 shows a 95% confidence interval of predicted link travel times and speeds against the ground truth at 07:00 to 23:00 on link 6. This link (i.e. OL6 in Fig. 3) is used for performance evaluation, and it is regarded as observed or unobserved in the latter analysis.

The MAPE, mean absolute error (MAE), and root mean square error (RMSE) are adopted for evaluating the performance of prediction results. The FPCA outputs in terms of travel times and speeds are summarized in Tables 2 and 3 respectively. The prediction error of the coefficient of variation of travel times and speeds (that is, the ratio between the mean and standard deviation of the travel times/speeds) is also provided in these two tables for comparison. As shown in Table 2, the prediction errors of both the mean and standard deviation of the link travel times vary considerably. The current experiments regard speed collected by point detectors as input for FPCA models at the link level. The performance may be different when converted link travel times from speeds are used as the input. The prediction errors of the path travel times are more significant than those of the link travel times. The errors for observed link 11 are the lowest in terms of both the mean and standard deviation. A site investigation has revealed that the speeds on link 11 are not less than 80 km/h for several days. The travel times on link 11 also vary slightly within a day. There are no congestions on link 11 compared with traffic conditions on link 6. Hence, the predicted link travel times/speeds on link 11 are more accurate. Overall, traffic conditions affect the prediction accuracy of link travel times and speeds.

In order to validate the results of stage 2 in the proposed prediction framework, an observed link 6 (i.e. OL6 in Fig. 3) is assumed to be unobserved, so that there are a total of six observed and eight unobserved links. Moreover, 2017 data, **excluding weekends and public holidays**, are also used to test the effects of the amount of historical data on the proposed prediction framework. Table 4 compares the prediction errors of the cases with link 6 as observed and unobserved. The case with link 6 as observed features smaller errors, as traffic data on the link are available for prediction. Moreover, the improvement in prediction

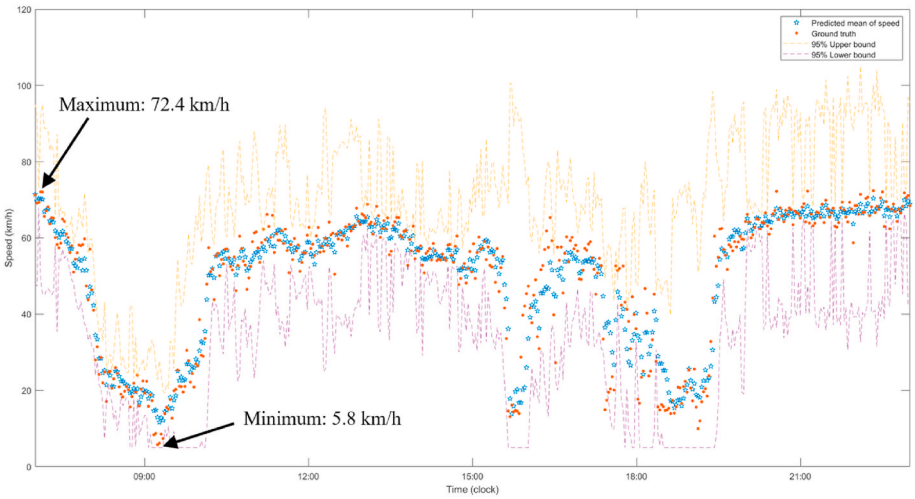

Fig. 7. 95% confidence interval of the predicted average speed of link 6 during 7:00–23:00.

Table 2
Results of prediction errors of path/observed link travel times, obtained by FPCA.

	Prediction errors of mean travel times			Prediction errors of standard deviation of travel times			Prediction errors of coefficient of variation of travel times		
	MAPE (%)	MAE (s)	RMSE (s)	MAPE (%)	MAE (s)	RMSE (s)	MAPE (%)	MAE	RMSE
Path	**5.4**	51.5	85.5	**18.9**	24.5	26.2	18.5	0.172	0.483
Link 1	3	2.6	5	16.3	13.1	22.6	15	0.962	2.442
Link 3	2.5	2	3.7	15.5	7	13.2	15.3	0.345	0.971
Link 5	3.5	4.8	9.2	18.5	16.2	26.7	**20**	1.081	2.494
Link 6	2.6	1.1	1.8	18.6	5	9.1	18.9	0.344	0.957
Link 8	2.4	1.4	2.1	15.7	3.9	6.6	15.3	0.178	0.374
Link 11	**0.5**	0.1	0.1	**8.4**	0.1	0.1	**8.6**	0.002	0.002
Link 12	1.4	0.4	0.7	9.1	0.9	2.7	9.8	0.019	0.093

Table 3
Results of prediction errors of path/observed link speeds, obtained by FPCA.

	Prediction errors of mean speeds			Prediction errors of standard deviation of speeds			Prediction errors of coefficient of variation of speeds		
	MAPE (%)	MAE (km/h)	RMSE (km/h)	MAPE (%)	MAE (km/h)	RMSE (km/h)	MAPE (%)	MAE	RMSE
Path	**6.9**	1.9	2.2	8.1	0.9	1.1	**6.8**	0.018	0.021
Link 1	4.3	1.5	1.8	**8.9**	0.8	0.8	5.6	0.007	0.008
Link 3	3.5	1.3	1.7	7.7	0.8	0.8	4.8	0.008	0.01
Link 5	5.4	1.4	2.8	8.8	0.6	0.8	5.4	0.006	0.013
Link 6	3.6	1	1.5	7.9	0.8	0.9	5.8	0.012	0.017
Link 8	3.5	1.2	1.4	8.3	0.9	1	6	0.014	0.017
Link 11	**0.7**	0.7	0.9	**4.1**	1.7	1.7	**3.3**	0.02	0.025
Link 12	1.7	1.2	1.6	4.4	1.1	1.1	3.3	0.009	0.012

Table 4
Comparison results of speed prediction errors between data with link 6 as observed or unobserved.

		Prediction errors of mean speeds			Prediction errors of standard deviation of speeds			Prediction errors of coefficient of variation of speeds		
		MAPE (%)	MAE (km/h)	RMSE (km/h)	MAPE (%)	MAE (km/h)	RMSE (km/h)	MAPE (%)	MAE	RMSE
Nov. 2017 data	Link 6 as observed	**3.6**	1	1.5	**7.9**	0.8	0.9	**5.8**	0.012	0.017
	Link 6 as unobserved	**18**	4.5	5.6	**15.9**	1	1.1	**12**	0.038	0.05
2017 data	Link 6 as observed	**1.9**	0.6	0.9	**6.3**	0.6	0.7	**4.3**	0.009	0.013
	Link 6 as unobserved	**14.8**	**3.9**	4.7	**12.1**	0.7	0.9	**10.4**	0.026	0.04

accuracy is limited when the historical data is extended from one month to one year for training purposes.

For comparison, other prediction models are also applied to this case study, including the long short-term memory neural network (LSTM NN) and autoregressive integrated moving average (ARIMA) models. Other state-of-art LSTM models, including attention-based LSTM models (Wu et al., 2020) and LSTM encoder–decoder models (Wang et al., 2021), are compared with use of the detector data collected in 2017, **excluding weekends and public holidays**. It can be seen in Table 5 that the proposed framework outperforms the other benchmark models with the lowest MAPE, MAE and RMSE.

Table 5
Path travel time prediction results of other benchmark models based on 2017 data.

Models	Prediction errors of path travel time		
	MAPE (%)	MAE (s)	RMSE (s)
(a) Proposed framework	**4.4**	42.1	75.1
(b) LSTM NN	6.1	55.8	85.2
(c) Attention-based LSTM (Wu et al., 2020)	5.9	53.6	77.3
(d) LSTM encoder–decoder model (Wang et al., 2021)	5.5	52	75.8
(e) ARIMA	7.1	62.4	93.1

5. Conclusion

This paper proposed a 2-stage short-term rolling horizon prediction framework (updated once every 2 min for the next 30 min) for predicting the travel time variations of both the observed and unobserved links along the study path using point detector data and JTIS estimates. Firstly, the path travel times and observed link travel times and their standard deviations were predicted in stage 1 with use of FPCA models. The stochastic processes of the current and predicting time horizons for the path and observed link travel time estimates were then modeled separately. It follows in stage 2 that the MLE model was applied to estimate the travel time variations of unobserved links along the study path.

A sensitivity test of the rolling horizon was conducted for selecting the appropriate rolling horizon scheme in the case study. With the rolling horizon of 60 min, the within-day predicted travel time variations of the study path, observed links, and unobserved links were evaluated using an independent dataset from JTIS. The MAPEs for the predicted mean travel times on the study path and observed links were less than 10%. Meanwhile, the MAPEs for the predicted standard deviation of the mean travel times were less than 20% at stage 1. In the case study, an observed link (i.e. OL6 in Fig. 3) was regarded as unobserved for evaluating the prediction performance at stage 2. It was found that the MAPEs for the predicted mean and standard deviation of travel times on the unobserved link were within 20%. The validation results are promising and demonstrate the practical applicability of the proposed prediction framework.

In the current approach, the rolling horizon was given and fixed for

the within-day travel time prediction. In the future, a self-adaptive rolling horizon scheme will be investigated through rolling horizon optimization. The within-day travel time variations can be examined by vehicle type, to obtain the short-term predicted travel time information for different vehicle types. Moreover, the prediction of day-to-day travel time variations will be further studied according to the prediction of within-day travel time variations. The effects of weather and road accidents on travel time/speed prediction may also be assessed in the future.

Declaration of competing interest

The authors declare that they have no known competing financial interests or personal relationships that could have appeared to influence the work reported in this paper. The authors declare the following financial interests/personal relationships which may be considered as potential competing interests:

Acknowledgments

This work was jointly supported by a postgraduate studentship from the Hong Kong Polytechnic University and grant from the Research Grants Council of the Hong Kong Special Administrative Region, China (Project No. PolyU R5029-18). The authors thank the Transport Department of the Government of the Hong Kong Special Administrative Region for providing the relevant traffic data for the research work.

References

Celikoglu, H.B., 2007. A dynamic network loading process with explicit delay modelling. Transport. Res. C Emerg. Technol. 15, 279–299. https://doi.org/10.1016/j.trc.2007.04.003.

Chen, K., Müller, H.G., 2014. Modeling conditional distributions for functional responses, with application to traffic monitoring via GPS-enabled mobile phones. Technometrics 56, 347–358. https://doi.org/10.1080/00401706.2013.842933.

Chiou, J.M., 2012. Dynamical functional prediction and classification, with application to traffic flow prediction. Ann. Appl. Stat. 6, 1588–1614. https://doi.org/10.1214/12-AOAS595.

Chiou, J.M., Zhang, Y.C., Chen, W.H., Chang, C.W., 2014. A functional data approach to missing value imputation and outlier detection for traffic flow data. Transport. Bus. 2, 106–129. https://doi.org/10.1080/21680566.2014.892847.

Cui, Z., Ke, R., Pu, Z., Ma, X., Wang, Y., 2020. Learning traffic as a graph: a gated graph wavelet recurrent neural network for network-scale traffic prediction. Transport. Res. C Emerg. Technol. 115, 102620 https://doi.org/10.1016/j.trc.2020.102620.

Dion, F., Rakha, H., 2006. Estimating dynamic roadway travel times using automatic vehicle identification data for low sampling rates. Transp. Res. Part B Methodol. 40, 745–766. https://doi.org/10.1016/j.trb.2005.10.002.

Du, L., Peeta, S., Kim, Y.H., 2012. An adaptive information fusion model to predict the short-term link travel time distribution in dynamic traffic networks. Transp. Res. Part B Methodol. 46, 235–252. https://doi.org/10.1016/j.trb.2011.09.008.

Ei Faouzi, N.-E., Billot, R., Bouzebda, S., 2010. Motorway travel time prediction based on toll data and weather effect integration. IET Intell. Transp. Syst. 4, 338. https://doi.org/10.1049/iet-its.2009.0140.

Feng, X., Ling, X., Zheng, H., Chen, Z., Xu, Y., 2019. Adaptive multi-kernel SVM with spatial-temporal correlation for short-term traffic flow prediction. IEEE Trans. Intell. Transport. Syst. 20 https://doi.org/10.1109/TITS.2018.2854913, 2001–2013.

Fusco, G., Colombaroni, C., Isaenko, N., 2016. Short-term speed predictions exploiting big data on large urban road networks. Transport. Res. C Emerg. Technol. 73, 183–201. https://doi.org/10.1016/j.trc.2016.10.019.

Gu, Y., Lu, W., Xu, X., Qin, L., Shao, Z., Zhang, H., 2020. An improved bayesian combination model for short-term traffic prediction with deep learning. IEEE Trans. Intell. Transport. Syst. 21, 1332–1342. https://doi.org/10.1109/TITS.2019.2939290.

Guardiola, I.G., Leon, T., Mallor, F., 2014. A functional approach to monitor and recognize patterns of daily traffic profiles. Transp. Res. Part B Methodol. 65, 119–136. https://doi.org/10.1016/j.trb.2014.04.006.

Hellinga, B., Izadpanah, P., Takada, H., Fu, L., 2008. Decomposing travel times measured by probe-based traffic monitoring systems to individual road segments. Transport. Res. C Emerg. Technol. 16, 768–782. https://doi.org/10.1016/j.trc.2008.04.002.

Hofleitner, A., Herring, R., Bayen, A., 2012. Arterial travel time forecast with streaming data: a hybrid approach of flow modeling and machine learning. Transp. Res. Part B Methodol. 46, 1097–1122. https://doi.org/10.1016/j.trb.2012.03.006.

Ji, H., Müller, H.G., 2017. Optimal designs for longitudinal and functional data. J. Roy. Stat. Soc. B Stat. Methodol. 79, 859–876. https://doi.org/10.1111/rssb.12192.

Lam, W.H.K., Shao, H., Sumalee, A., 2008. Modeling impacts of adverse weather conditions on a road network with uncertainties in demand and supply. Transp. Res. Part B Methodol. 42, 890–910. https://doi.org/10.1016/j.trb.2008.02.004.

Li, H., Li, M., Lin, X., He, F., Wang, Y., 2020. A spatiotemporal approach for traffic data imputation with complicated missing patterns. Transport. Res. C Emerg. Technol. 119, 102730 https://doi.org/10.1016/j.trc.2020.102730.

Li, R., Rose, G., 2011. Incorporating uncertainty into short-term travel time predictions. Transport. Res. C Emerg. Technol. 19, 1006–1018. https://doi.org/10.1016/j.trc.2011.05.014.

Li, W., Wang, J., Fan, R., Zhang, Y., Guo, Q., Siddique, C., Ban, X., Jeff), 2020. Short-term traffic state prediction from latent structures: accuracy vs. efficiency. Transport. Res. C Emerg. Technol. 111, 72–90. https://doi.org/10.1016/j.trc.2019.12.007.

Lu, L., Wang, J., He, Z., Chan, C.Y., 2018. Real-time estimation of freeway travel time with recurrent congestion based on sparse detector data. IET Intell. Transp. Syst. 12, 2–11. https://doi.org/10.1049/iet-its.2016.0356.

Mori, U., Mendiburu, A., Álvarez, M., Lozano, J.A., 2015. A review of travel time estimation and forecasting for Advanced Traveller Information Systems. Transportmetrica: Transport. Sci. 11, 119–157. https://doi.org/10.1080/23249935.2014.932469.

Müller, H.G., Yao, F., 2008. Functional additive models. J. Am. Stat. Assoc. 103, 1534–1544. https://doi.org/10.1198/016214508000000751.

Papageorgiou, M., Papamichail, I., Messmer, A., Wang, Y., 2010. Traffic simulation with METANET. https://doi.org/10.1007/978-1-4419-6142-6_11, pp. 399-430.

Shao, H., Lam, W.H.K., Sumalee, A., Chen, A., 2018. Network-wide on-line travel time estimation with inconsistent data from multiple sensor systems under network uncertainty. Transportmetrica: Transport. Sci. 14, 110–129. https://doi.org/10.1080/23249935.2017.1323039.

Shao, H., Lam, W.H.K., Sumalee, A., Chen, A., 2013. Journey time estimator for assessment of road network performance under demand uncertainty. Transport. Res. C Emerg. Technol. 35, 244–262. https://doi.org/10.1016/j.trc.2012.12.002.

Soriguera, F., Robusté, F., 2011. Highway travel time accurate measurement and short-term prediction using multiple data sources. Transportmetrica 7, 85–109. https://doi.org/10.1080/18128600903244651.

Tam, M.L., Lam, W.H.K., 2011. Application of automatic vehicle identification technology for real-time journey time estimation. Inf. Fusion 12, 11–19. https://doi.org/10.1016/j.inffus.2010.01.002.

Tam, M.L., Lam, W.H.K., 2008. Using automatic vehicle identification data for travel time estimation in Hong Kong. Transportmetrica 4, 179–194. https://doi.org/10.1080/18128600808685688.

Vlahogianni, E.I., Karlaftis, M.G., Golias, J.C., 2014. Short-term traffic forecasting: where we are and where we're going. Transport. Res. C Emerg. Technol. 43, 3–19. https://doi.org/10.1016/j.trc.2014.01.005.

Wang, W., 2015. Link Travel Time Estimation Based on Network Entry/exit Time Stamps of Trips. Texas A&M University.

Wang, Z., Su, X., Ding, Z., 2021. Long-term traffic prediction based on LSTM encoder-decoder architecture. IEEE Trans. Intell. Transport. Syst. 22, 6561–6571. https://doi.org/10.1109/TITS.2020.2995546.

Wu, P., Huang, Z., Pian, Y., Xu, L., Li, J., Chen, K., 2020. A combined deep learning method with attention-based LSTM model for short-term traffic speed forecasting. J. Adv. Transport. https://doi.org/10.1155/2020/8863724, 2020.

Xiao, Y., 2011. Hybrid Approaches to Estimating Freeway Travel Times Using Point Traffic Detector Data. Florida International University. https://doi.org/10.25148/etd.FI11042503.

Yang, G., Wang, Y., Yu, H., Ren, Y., Xie, J., 2018. Short-term traffic state prediction based on the spatiotemporal features of critical road sections. Sensors 18, 2287. https://doi.org/10.3390/s18072287.

Yao, F., Müller, H.G., Wang, J.L., 2005. Functional data analysis for sparse longitudinal data. J. Am. Stat. Assoc. 100, 577–590. https://doi.org/10.1198/016214504000001745.

Yildirimoglu, M., Geroliminis, N., 2013. Experienced travel time prediction for congested freeways. Transp. Res. Part B Methodol. 53, 45–63. https://doi.org/10.1016/j.trb.2013.03.006.

Yin, H., Wong, S.C., Xu, J., Wong, C.K., 2002. Urban traffic flow prediction using a fuzzy-neural approach. Transport. Res. C Emerg. Technol. 10, 85–98. https://doi.org/10.1016/S0968-090X(01)00004-3.

Yin, K., Wang, W., Bruce Wang, X., Adams, T.M., 2015. Link travel time inference using entry/exit information of trips on a network. Transp. Res. Part B Methodol. 80, 303–321. https://doi.org/10.1016/j.trb.2015.07.007.

Zhong, R.X., Luo, J.C., Cai, H.X., Sumalee, A., Yuan, F.F., Chow, A.H.F., 2017. Forecasting journey time distribution with consideration to abnormal traffic conditions. Transport. Res. C Emerg. Technol. 85, 292–311. https://doi.org/10.1016/j.trc.2017.08.021.

Zhong, R.X., Xie, X.X., Luo, J.C., Pan, T.L., Lam, W.H.K., Sumalee, A., 2020. Modeling double time-scale travel time processes with application to assessing the resilience of transportation systems. Transp. Res. Part B Methodol. 132, 228–248. https://doi.org/10.1016/j.trb.2019.05.005.